



ISSN: 0067-2904

Classification and Measurement of Land Cover of Wildfires in Australia Using Remote Sensing

Assad H. Thary Al-Ghraiiri^{1*}, Enas Kh. Hassan², Harith M. Saeed³

¹Department of Computer Science, College of Science, Al-Nahrain University, Baghdad, Iraq,

²Department of Computer Science, College of Science, University of Baghdad, Baghdad,

³Department of Physics, College of Science, Al-Nahrain University, Baghdad, Iraq,

Received: 26/4/2021

Accepted: 28/6/2021

Abstract

Remote sensing techniques used in many studies for classifying and measuring of wildfires. Satellite Landsat8(OLI) imagery is used in the presented work. The satellite is considered as a near-polar orbit, with a high multispectral resolution for covering Wollemi National Park in Australia. The work aims to study and measure wildfire natural resources prior to and throughout fire breakout which occurred in Wollemi National Park in Australia for a year (October, 2019), as well as analyzing the harm resulting from such wildfires and their effects on earth and environment through recognizing satellite images for studied region prior to and throughout wildfires. A discussion of methods for computing the affected area is covered regarding each one of the classes and lessening or limiting the quickly-spreading wildfires damage. This paper propose a 2-phases techniques: training and classifying. In the training phase, the number of clustering is computed by using C# Programming Language and feature extracted and clustered as a group and stored in the dataset. The classification used the moments with (K-Means) classification approach in RS (Remote Sensing) for classified image. The results of classification showed 5 distinctive classes (trees, rivers, bare earth, buildings with no trees, and buildings with trees) in which it might be indicates that the region is secured via each one of the classes prior to and throughout wildfires as well as the changed pixels with regard to all the classes. Also, the classification experimental methods results indicate an excellent performance recision with a good classifying and result analysis about the harms caused by fires in the study area.

Keywords: Landsat-8(OLI), Moment feature, Wollemi National Park, Unsupervised Classifying Image, Remote sensing Techniques.

تصنيف وقياس الغطاء الأرضي لحرائق الغابات في أستراليا باستخدام الاستشعار عن بعد

أسد حسين ذاري^{1*}, إيناس خزعل حسن², حارث محمد سعيد³

¹قسم علوم الحاسوب، كلية العلوم، جامعة النهرين، بغداد، العراق

²قسم علوم الحاسوب، كلية العلوم، جامعة بغداد، بغداد، العراق

³قسم الفيزياء، كلية العلوم، جامعة النهرين، بغداد، العراق

*Email: Enas.mkhazal@gmail.com

الخلاصة

تم استخدام صور القمر الصناعي Landsat8 في العمل المقدم ؛ يعتبر القمر الصناعي مدارًا شبه قطبي ، مع دقة عالية متعددة الأطياف لتغطية متنزه Wollemi الوطني في أستراليا. يهدف العمل إلى دراسة وقياس الموارد الطبيعية لحرائق الغابات قبل وخلال اندلاع الحريق الذي حدث في Wollemi National Park في أستراليا في عام (2019) ، وكذلك تحليل الضرر الناتج عن حرائق الغابات وتأثيراتها على الأرض والبيئة. من خلال التعرف على صور الأقمار الصناعية للمنطقة المدروسة قبل حرائق الغابات وخلالها ومناقشة طرق حساب المنطقة المغطاة فيما يتعلق بكل فئة من الفئات وتقليل أو الحد من أضرار حرائق الغابات سريعة الانتشار. تشتمل التقنيات المقترحة في هذه الورقة على مرحلتين: التدريب والتصنيف ؛ في مرحلة التدريب ، يتم حساب عدد المجموعات واستخراج الميزة والتجميع كمجموعة ومخزن في مجموعة البيانات. استخدم التصنيف للحظات مع منهج التصنيف (K-Means) في RS (الاستشعار عن بعد) للصورة المصنفة. أظهرت نتائج التصنيف 5 فئات مميزة (الأشجار ، الأنهار ، الأرض المكشوفة ، المباني الخالية من الأشجار ، المباني بالأشجار) والتي يمكن الإشارة فيها إلى أن المنطقة مؤمنة من خلال كل فئة من الفئات قبل وخلال حرائق الغابات وكذلك وحدات البكسل المتغيرة فيما يتعلق بجميع الفئات. كما أشارت النتائج التجريبية لطريقة التصنيف إلى مراجعة أداء ممتازة مع تصنيف جيد وتحليل للنتائج للأضرار التي تسببها الحرائق في منطقة الدراسة.

1. Introduction

Throughout history, land is one of the major natural sources. Land cover refers to the characteristics that cover the earth as represented by natural elements such as vegetation regions, rivers, bare earth, impermeable surface, and other earth's physical characteristics. The land surface is a combination of natural and human factors, including vegetation, soil, ice & glaciers, lakes, wetlands, and a variety of urban cities [1]. Remote sensing technologies were used in the past decades for studying land surface and earth observation for surveying amount of the distribution regarding natural resources of the earth [2]. Also, remote sensing was advanced in the temporal, spatial, and spectral resolutions for using satellite imagery to choose the area, understanding, mapping, evaluations, error modulation, and accurate computation of images [3]. Land use and land surface classification are very important because they provide information vital for assessing and monitoring natural resources in different geographical locations [4]. Land use relates to human-induced modifications for agricultural, industrial, residential, or recreational purposes; land use describes how individuals use the land for socio-economic reasons; agricultural and urban land use were 2 of the major high-level groups of users. Data on land surface and land use are highly important for the decision-makers, planners, and individuals that are interested in management of land resources [2]. To make use of analysis and monitoring of the urban environment, they should develop [3], Land Use and Land Cover (LULC) information with regard to sustainable and proficient management of urban areas. Each one of the land parcels on the earth's surface was distinctive in the cover it possesses [4]. Image classification is an excellent strategy for preparing digital images for information in land cover to extract and use data in remotely-sensed images. The classes were identified into specified relevant classes (water, bare earth, trees, buildings with trees, and buildings with no trees) [4][5][6]. Image classification is when decision rules are developed and used to assign pixels into classes with similar spectral and information features [6]. Satellite image classification is utilized to extract spectral signature from the satellite images as well as analyzing the land-cover map of a selected area [7][8][9]. The techniques of classification can be categorized into 2 types: supervised and unsupervised [10][11]. The work aims to study and measure the wildfire natural resources prior to and throughout fire breakout which occurred in Wollemi National Park in Australia in year (2019). The approach of the moment feature clustering has been deployed as unsupervised

form of the classification for Australian Wollemi National Park for the classification of wildfire, dangerous threats and damages, which have happened in the area. The remaining parts of the present study can be given as follows: Section 2 explains study area and description. Section 3 explains the methodology. Section 4 presents the diagram of the system with approaches of image classification. Section 5 includes a description of experimental results and result measurements. Ultimately, conclusions and future work suggestions were given in Section 6.

2. Study area and description

In this work, the position of study is shown in Figure 1 Wollemi National Park in Australia country, which have been captured by Landsat-8 with three color bands by a 30m resolution in the year 2019.



Figure 1-The location of area study in Australia

There were many researches taken into account the handling of satellite images as well as knowing the subtleties, also exploiting gigantic data of the images [12][13][14][15][16] [17]. The data is used for predicting future environmental changes or disasters in climate conditions and many things in daily matters. There are portions of previous studies which were examined in this field. A study conducted by [13] showed the Forest Fire Damage Estimation with the use of GIS and remote sensing. A study conducted by [18] shows the classification of the objects according to the development of proceedings of classification for the burning area map and some fire damages that have happened from the summer of (2007) to the summer of (2009) in Greece, via the presentation of the pour system” observation de la Terre (SPOT4) HRVIR images”. In [19][20][21], have presented a classification of the satellite imagery environments using a creative approach that has been referred to as the RBPM (i.e. the Reflection Based Phenology Method), in which Landsat 8 datasets were utilized, keeping the image in the multi-spectral. The band reflection basis of the values has been used in the procedure of the classification. In [22][23], Stated a proposal of a method of classification that has been utilized for discovering the classes of the land cover in the satellite imagery.

3. Methodology

One of most important aspects of utilizing the region of Wollemi National Park in Australia is the wildfires causing huge problems in this region and has (5 kinds of lands) and being utilized as support for understanding. Those classes are the trees region, rivers, buildings with trees, bare earth and buildings without trees. The regions where the fire happens have been specified through the use of the approaches for the classification of the fire and discuss the impacts of the wildfire upon every one of the areas that are covered with every one of the classes. Satellite images of this region has been captured by the (Landsat8) with a 30m resolution prior to and throughout wild-fire.

4. The Suggested Approaches of Classification

Features of the homogeneous regions in an image may be classified through the use of visual perception elements. The classifying method may be supervised as well as unsupervised to be relegated to a defined class dependent upon the amount of the feature's extraction identified with the image [22]. A satellite imagery includes several characteristics, such as, the remote sensing casing for spectral area, and each signature property is present in separate class [24]. In supervised classification; classes can be seen through giving an analyzed information group sample to an administrator [17]. Moments that are based upon the K-mean have been used for the extraction of all the features and classifying the image. Figure 2 illustrates the ideas of the suggested approach for the classification.

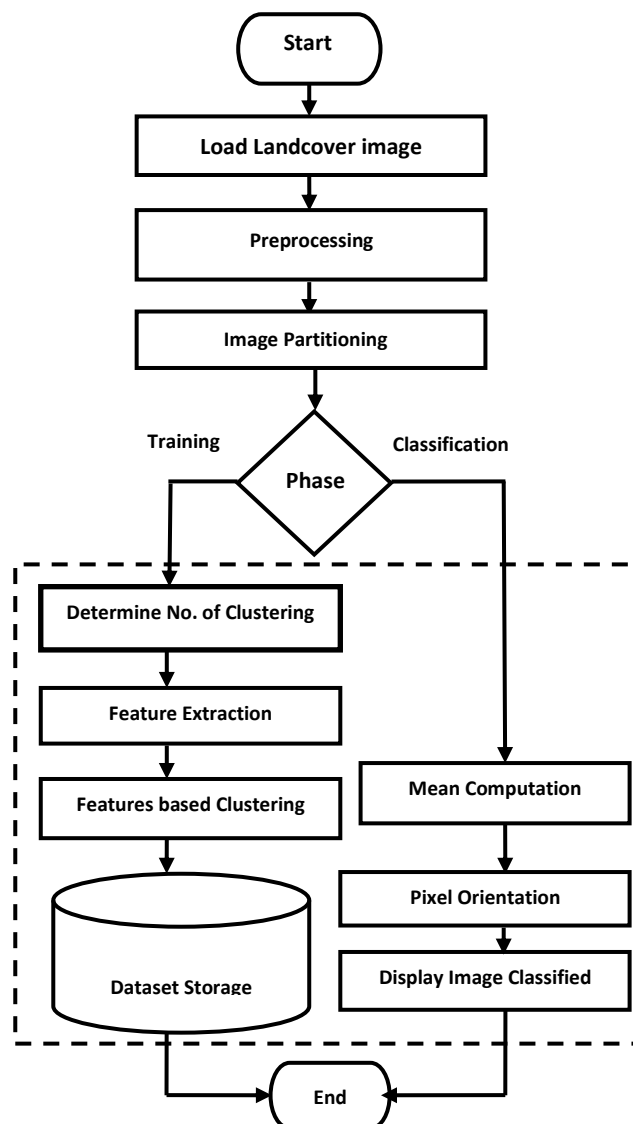


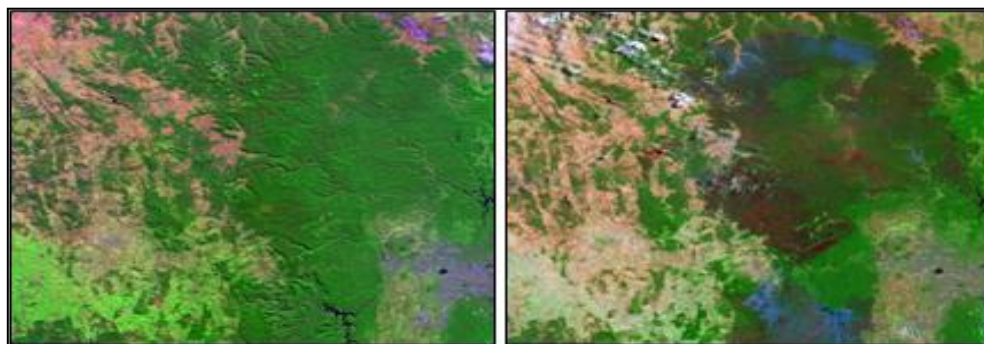
Figure 2-Block diagram of Classify Satellite image.

4.1 Imagery of the Load Landcover (LC)

Satellite Landsat-8 OLI Sensor imagery can be defined as a multi-spectral high-resolution near-polar-orbiting, with the aim of covering the National Park of Wollemi. This image has been captured by Landsat-8 OLI Sensor with a 30 m resolution. It covers wild-fires (i.e. the natural resources) prior to and during the wildfire break out that had occurred in the region in the year (2019). Table 1 lists technical data on original images as well as original satellite images of the Wollemi Park prior to and throughout the wildfires for October, 2019 have been illustrated in Figure 3.

Table 1-The technical information on the original images

Products	Satellites/Sensors	Resolution	Date of Acquisition:	Band name	Band Combination that has been utilized for the creation of that image:	Wavelength (µm)
Format of Geo Tiff	Landsat 8 OLI	30 meters	31 Dec 2019 & 24 Jul 2019	SWIR 2, NIR, Blue	7, 5, 2 (false color) RGB	(2.11 - 2.29), (0.85 - 0.88), (0.45 - 0.51)



a. Wollemi National Park - before Fires. b. Wollemi National Park - during Fires.

Figure 3-The images represent Wollemi National Park in Australia before and during Wildfires for 2019.

4.2 Pre-processing

The pre-processing has been utilized in the present study in order to upgrade the considered images visual appearance. This process is relied on focusing every pixel without an impact on contiguous correlation pixels and enhancing recognition between image highlights by the application of the following connection upon an image [19]:

$$Ge(x,y)=round[(Go(x,y) -h) / (h-l)*255] \quad \dots (1)$$

Ge(x,y) refers to new upgraded image, Go(x,y) represents (original image), and x&y refers to the pixel location in the image. (h) represents top (1%) for pixels estimations of (original image), and (l) indicates to bottom (1%) of pixels estimations of (original images) [25]. The image segmentation may be defined as a process of dividing that image to uniform-sized block squares (Mask). And it has been found that the process is not concerned with spectral image scattering; it is simply partitioned according to RASTER Model. In the present study, each square size is (4x4) block size where it has been dependent upon the spatial image resolution measure, where lower resolution of image has been separated into a squared

number less compared to the higher resolution of the image. For the purpose of adopting proper data has been contained in each mask.

4.3 Number of Clustering Computation

In this step, the number of clustering in the original image is calculated in the following steps:

1. Compute the number of pixels in original image (N_P) with the use of the following equation:

$$N_P = w \times h \quad \dots (2)$$

2. Determine the standard deviation (σ) by the following:

$$\sigma = \sqrt{\frac{1}{N_P} \sum_{i=0}^{w-1} \sum_{j=0}^{h-1} (G_P(i, j) - \overline{G_P})^2} \quad \dots (3)$$

Where $\overline{G_P}$ is the mean of the original image as shown in the equation below:

$$\overline{G_P} = \frac{1}{N_P} \sum_{i=0}^{w-1} \sum_{j=0}^{h-1} G_P(i, j) \quad \dots (4)$$

3. Determine the number of the pixels (N) in an image falling in a 2σ range.

4. Calculate the percent (P) with the use of the equation:

$$P = \frac{N}{N_P} \quad \dots (5)$$

5. The number of the classes (N_C) has been equal to multiplying the percentage (P) by maximal likely number (P_M) of the classes can be discovered in satellite images according to:

$$N_C = P \times P_M \quad \dots (6)$$

4.4 Feature Extract and Clustering

The moments may be utilized for the differentiation of the images as an estimation, which depends upon their color highlights [23]. The characteristics of the moment may be characterized as a specific quantitative measurement, which has been utilized for the extraction of dataset in every one of the image masks. Where a mass would be alluding to a pixel set distribution, the (1st ordered moment) which can be calculated from the equation 2 has been used for the extraction of moment characteristics.

$$M = d \times G_P \quad \dots (7)$$

GP represents the applied force, which may be referred to as the block pixel, and distance may be referred to as d from the block center to applied force. The following steps describe how the distance is computed:

determined the distance (Ds) that average (between every one of the pixels in exact mask and mask center) and depends upon the pixel position with the use of:

In this equation, the 1st quarter distance (d) can be computed with the following eq.:

$$d1 = \sqrt{(|q - q_o| - 0.5)^2 + (|z - z_o| - 0.5)^2} \quad \dots (8)$$

In this equation, the 2' s quarter distance (ds2) has been determined by the utilization of the equation below:

$$d2 = \sqrt{(|q - q_o| - 0.5)^2 + (|z - z_o| + 0.5)^2} \quad \dots (9)$$

In this formula, the 3' s quarter distance (ds3) has been specified by utilizing Eq. 10.:

$$d3 = \sqrt{(|q - q_o| + 0.5)^2 + (|z - z_o| + 0.5)^2} \quad \dots (10)$$

Ultimately, this formula is the 4's quarter distance (ds4) that may be calculated with the use of Eq. 11:

$$d4 = \sqrt{(|q - q_o| + 0.5)^2 + (|z - z_o| + 0.5)^2} \quad \dots (11)$$

(q, z) represent the pixels in a square and (q, z) represents the locations of the square of center.

the feature moment of pixel GMP (q, z) can be calculated in a certain square in the image equation below:

$$GMp(q, z) = GP(q, z) \times d \quad \dots (12)$$

The certain mask (M) moment features an image may be calculated by using the relation below:

$$M(q,z) = \frac{1}{B_h \times B_w} \sum_{q=0}^{B_h} \sum_{z=0}^{B_w} M_p(q,z) \quad \dots (13)$$

Where B_w represents the mask width, and B_h refers to mask height, and $G_p(q, z)$ refers to value pixel of chosen mask. $(q&z)$ represent the locations of the pixel in the chosen image mask.

In the stage of the Clustering, K-Means method has been utilized through 2 input parameters, the 1st is values of the moment feature of each one of the image squares, and the 2nd is the amount of the classes (or the clusters). The feature of the moment is obtained for every one of the image squares and put away in 2-D array, and K-Mean approach has been implemented and all of those highlights have been gathered for the purpose of getting the optimal features (i.e. centroids). Where estimation of image pixels is part of every one of the centroids have been put away as a data-base vector, which has been used for the classification of the images.

4.5. Satellite Image Classification (Pixel Orientation)

The classifying stage is usually performed after the clustering of blocks and stored in a database. Classifying technique depends on examination of spectring amount to each pixel in built up dataset storage, according to nearness for each one of the pixels to the accessible classes in the dataset. The method of the classification has been performed through deciding the estimation of the similarity (S_m) between each one of the image pixels G_{xy} and average μ through the application of eq14. The maximum value S_m is an image estimation pixel for any of the classes [25].

$$S_m = 1 - |\mu - G_{xy}| \quad \dots (14)$$

5. Experiments And Measurement

A very significant factor of using Wollemi National Park in Australia before and during Wildfires in the year 2019 images is to have 5 types of features and being used as a tool that helps in explanations. It had discussed variations between the classes and the region which has been secured by every one of the classes has been studied. Images that have been captured by the (Land sat-8), which is a multi-spectral, near-polar-orbiting high-resolution satellite that covers Australia. In the present study, input images have been categorized prior to and throughout Wild-fires during October, 2019. Where, spectral highlight variations in those images have given 5 classes, which are: (trees, Rivers, buildings with trees, bare earth and buildings without trees). After the application of the approach of the classification, dataset includes the estimations of the moment feature element for the image squares that are similar for end best centroids that have been resulted from the application of (K-Mean) algorithm upon image masks, in which the number of the iterations that are expected to be getting assembled as well as the optimal centroids before and during Wildfires in the image of the Wollemi National Park in Australia that has been illustrated in Figure 3 (a&b) are (16, 12) respectively in (2019). The optimal 5 centroids represent feature for certain masks in the classified images. Figures (4&5) are the optimal centroids for classified image prior to and throughout Wildfire. Simultaneously, area (A) covered with every one of the classes in the classified images that may be specified through the use of eq. 10

$$A (m^2) = \text{Number of the Pixels} \times 30^2 \quad \dots (15)$$

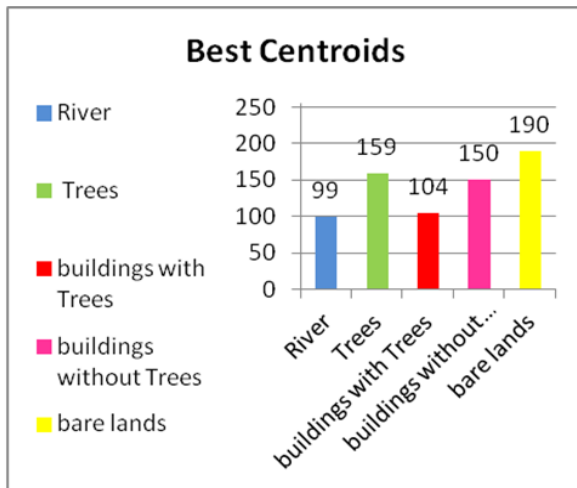


Figure 4. Five classes with the best Centroids before fires.

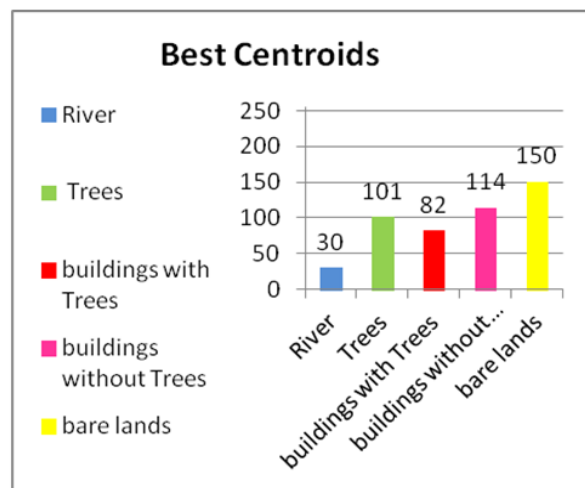


Figure 5. Five classes that have optimal Centroids throughout the fires.

The classifying results of the Wollemi National Park in Australia images before and following the (Wild-fires) in (2007) are shown in Figure 6: it is noticed there are five unique classes. The experimental results, as shown in Tables 2,3, respectively, clarified the area covered with each one of the classes prior to and throughout the Wildfire with the number of pixels for each class has been changed and the damages that have resulted from those wildfires have been detected and their effects upon the soil and environment have been assessed.

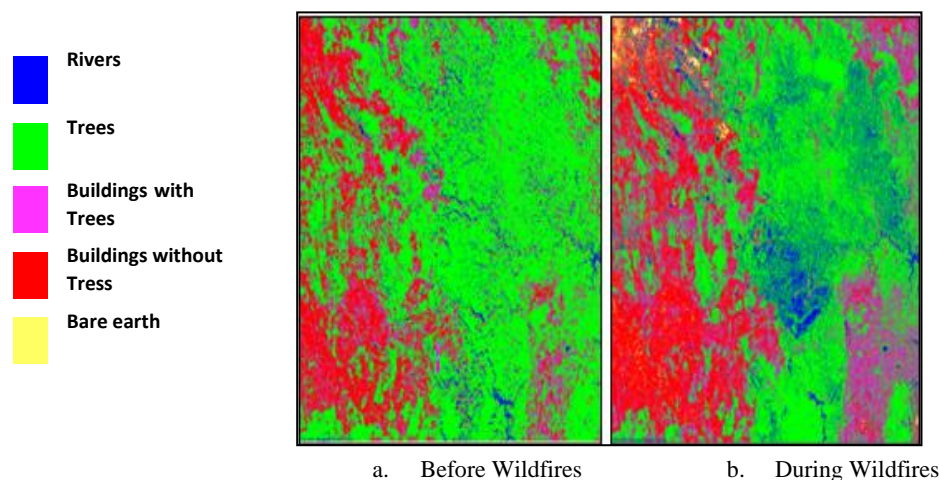


Figure 6- The classified images of Wollemi National Park in Australia before and during Wildfires for a year 2019.

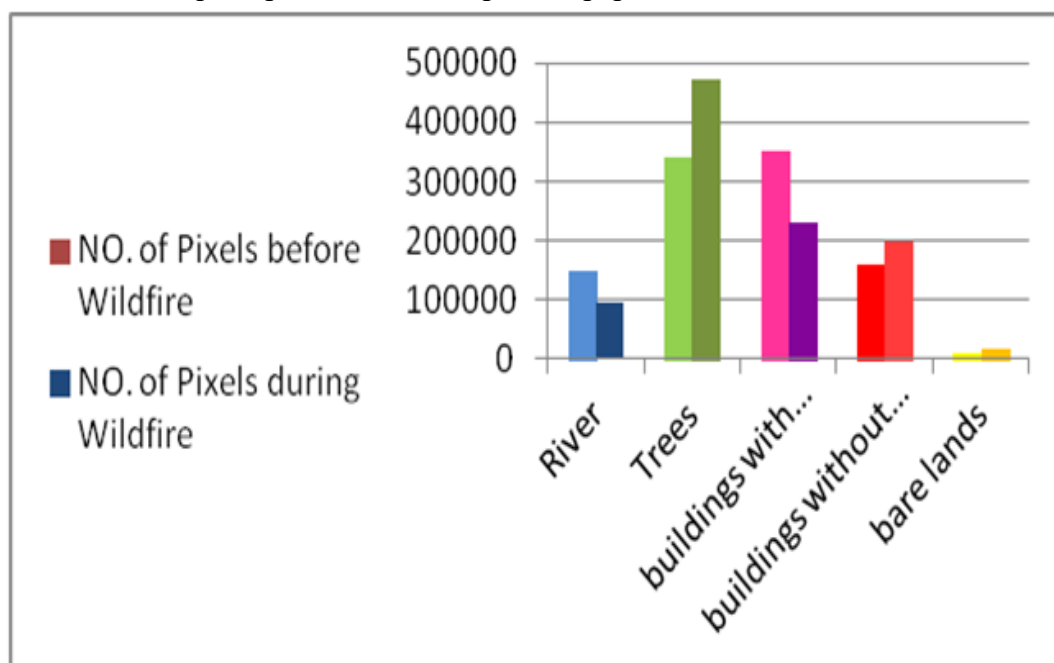
Table 2-The cover area and No. of pixel for each class in classified image before the wildfire

Classes	No. Pixels	Area Covers (m ²)
Rivers	149821	4494630
Tree area	471356	1.414068E+07
Buildings with trees	350789	1.052367E+07
Buildings without trees	158380	4751400
Bare earths	10251	307530

Table 3-The cover area and No. of pixel for each class in the classified image during a wildfire

Classes	Number of the Pixels	Area Covers (m ²)
Rivers	93755	2812650
Tree area	341447	1.024341E+07
Buildings with trees	231743	6952290
Buildings without trees	197585	5927550
Bare earth	16249	487470

The experimental resulted of the classifying technique presents that good performance the accuracy of image classified taken by Landsat-8 satellite and give good analysis results and measurements about the damages as shown in Figure 7, which represent the variation between each class before and during the wildfires. The tree class covers the region (1.414068E+07m² prior to the Wild-fires), whereas (during Wildfire it covered the region 1.024341E+07 m²). Otherwise, the number of pixels of building with trees class is 350789 before Wildfires), while (during Wildfires it is 231743) that refers to the size of harm. In addition to that, (bare earth class covered an area of 307530m² prior to the Wildfire), however, (throughout Wildfires, it has covered 487470m²). The observed from result analyses on harms that had happened due to wildfires in which the number of the pixel for the classes (trees and buildings with) have been diminishing throughout the (wild-fires) implying that the suggested classification technique's precision for the present paper have been studied.

**Figure 7**-The effects on the amount of the pixels for every one of the classes in the classified image

Prior to and throughout the Wildfire

6. Conclusions

Satellite Landsat-8 OLI sensor imagery is a near-polar-orbiting, multispectral high-resolution to cover the Wollemi National Park in Australia. The results of this work indicate that the influenced region, the burned regions. It observed every class impact before and during the wildfires that occurred in National park in Australia on October, 2019. The experimental results showed a good performance accuracy in classifying five different classes (rivers, trees, buildings with tree, buildings without tree, bare earth) and good result analysis and measurements about the damages resulting from the wildfires. The amount of the pixel for the class (trees as well as buildings with the trees) has been reduced throughout the (wildfire), meaning that the suggested method of the classification has been the optimal, concerning for the future works that have satellite imagery for this research, an identical location of the SVM or the GA classification.

References

- [1] GM Munna, SR Sourav, Al-Imran and R.K. Roy, "Land Use/Land Cover Change of Sylhet City using Remote Sensing and GIS", *Journal of Engineering and Applied Sciences*, vol. 15, no. 13, pp. 2734-2739, 2020.
- [2] Abbas, H., & George, L. E., "Image Classification Schemes Based on Sliced Radial Energy Distribution of DFT and the Statistical Moments of Haar Wavelet," *Iraqi Journal of Science*, vol. 61, no. 3, pp. 687-712, 2020, <https://doi.org/10.24996/ij.s.2020.61.3.25>.
- [3] Fadel Abbas Zwain, Thair Thamer Al-Samarrai, & Younus I. Al-Saady, "A Study of Desertification Using Remote Sensing Techniques in Basra Governorate, South Iraq," *Iraqi Journal of Science*, vol. 62, no. 3, pp. 912-926, 2021, <https://doi.org/10.24996/ij.s.2021.62.3.22>.
- [4] Patino, Jorge E., and Juan C. Duque. "A review of regional science applications of satellite remote sensing in urban settings," *Computers, Environment and Urban Systems*, vol. 37, pp. 1-17, 2013.
- [5] Mohammed, Ali Abdulwahhab, and Hussein Thary Khamees, "Categorizing and measurement satellite image processing of fire in the forest greece using remote sensing," *Indonesian Journal of Electrical Engineering and Computer Science*, vol. 21, no. 2, pp 843-853, 2021.
- [6] Jog, Sayali, and Mrudul Dixit, "Supervised classification of satellite images," In 2016 Conference on Advances in Signal Processing (CASP), pp. 93-98. IEEE, 2016.
- [7] Assad H. Thary Al-Ghraiiri, Mohammed S. Mahdi Al-Taei, "KMeans based SVD for Multiband Satellite Image Classification," *International Journal of Scientific & Engineering Research*, vol. e 7, Issue 8, ISSN 2229-5518, August-2016.
- [8] R. Mohamed et al., "Bat algorithm and k-means techniques for classification performance improvement," *Indonesian Journal of Electrical Engineering and Computer Science*, vol. 15, no. 3, pp. 1411-1418, September 2019.
- [9] Lu, D. and Weng Q., "A survey of image classification methods and techniques for improving classification performance," *International Journal of Remote Sensing*, vol. 28, no. 5, pp. 823-870, 2007.
- [10] Assad H. Thary Al-Ghraiiri, Hussein Thary Khamees, Ali A. Mohammed, Harith M.Saeed, Walaa S. Tahlok, Zahraa H. Abed, "Classify and Analysis of Fire in the Forest Greece Using Remote Sensing," *International Journal of Scientific & Engineering Research*, vol. 10, Issue 10, pp. 1364-1371, October-2019.
- [11] Ablin, R., C. Helen Sulochana, and G. Prabin, "An investigation in satellite images based on image enhancement techniques," *European Journal of Remote Sensing*, pp 1-9. 2019.
- [12] S. Manthira Moorthi, Indranil Misra, "Kernel based learning approach for satellite image classification using support vector machine," *Recent Advances in Intelligent Computational Systems (RAICS)*, IEEE, DOI: 10.1109/RAICS.2011.6069282, ISBN: 978-1-4244-9478-1, 03 November 2011.
- [13] Mohammed S. Mahdi Al-Taei, Assad H. Thary Al-Ghraiiri, "Satellite Image Classification Using Moment and SVD Method," *International Journal of Computer*, vol. 23, no. 1, pp. 10-34, 2016.

- [14] Hnatushenko, Vik V., Vik Hnatushenko, D. K. Mozgovyi, and V. V. Vasiliev, "Satellite Technology of the forest fires Effects Monitoring," *Scientific Bulletin of National Mining University*, vol. 1, 2016.
- [15] Vilar, Lara, Andrea Camia, and Jesús San-Miguel-Ayanz, "A comparison of remote sensing products and forest fire statistics for improving fire information in Mediterranean Europe," *European Journal of Remote Sensing*, vol. 48, no. 1, pp. 345-364. 2015.
- [16] Assad H. Thary Al-Ghraiiri, "Satellite Image Classification Using K-Means and SVD Techniques," LAP LAMBERT Academic Publishing ISBN: 978-620-2-02145-6, August 23, 2017.
- [17] Ugur Alganci, Elif Sertela, And Cankut Ormeci, "Forest Fire Damage Estimation Using Remote Sensing and GIS," *Remote Sensing for Science, Education, Raine Reuter (Editor) and Natural and Cultural Heritage*, 2010.
- [18] Anastasia Polychronaki and Ioannis Z. Gitas, "Burned Area Mapping in Greece Using SPOT-4 HRVIR Images and Object-Based Image Analysis," *Remote Sens.*, pp. 424-438, 2012.
- [19] Aliyu, Hajara Abdulkarim, Mohd Azhar Abdul Razak, and Rubita Sudirman. "Normal and abnormal red blood cell recognition using image processing," *Indonesian Journal of Electrical Engineering and Computer Science*, vol. 14, no. 1, pp. 100-104, 2019.
- [20] Florin-Andrei Georgescu, Corina Vaduva, Dan Raducanu, and Mihai Datcu, "Feature Extraction for Patch-based Classification of Multispectral Earth Observation Images," Published in *IEEE*, vol. 13, Issue, 6, June 2016.
- [21] Gure, Mulayim, Mehmet Emin Ozel, H. Hulya Yildirim, and Muzaffer Ozdemir, "Use of satellite images for forest fires in area determination and monitoring," In 2009 4th International Conference on Recent Advances in Space Technologies, pp. 27-32. IEEE, 2009.
- [22] Abburu, Sunitha, and Suresh Babu Golla, "Satellite image classification methods and techniques: A review," *International journal of computer applications*, vol. 119, no. 8, 2015.
- [23] Rahul Neware, Amreen Khan, "Survey on Classification techniques used in remote sensing for satellite images," ResearchGate, March 2018.
- [24] Parameswaran, Namboodiri Sandhya, and D. Venkataraman, "A computer vision based image processing system for depression detection among students for counseling," *Indones. J. Electr. Eng. Comput. Sci*, vol. 14, no. 1, pp 503-512. 2019.
- [25] Assad H. Thary Al-Ghraiiri, Zahraa H. Abed, Fatimah H. Fadhil, Faten K., "Classification of Satellite Images Based on Color Features Using Remote Sensing," *International Journal of Computer*, vol. 31, no 1, pp. 42-52, 2018.